Sensitivity of fast ion losses to magnetic perturbations in the European DEMO

J. Varje[a], T. Kurki-Suonio[a], A. Snicker[a,b], K. Särkimäki[a], P. Vincenzi[c], P. Agostinetti[c], E. Fable[b], P. Sonato[c], F. Villone[d]

[a]*Department of Applied Physics, Aalto University, FI-00076 AALTO, Finland*
[b]*Max-Planck-Institut für Plasmaphysik, Garching, Germany*
[c]*Consorzio RFX Corso Stati Uniti 4 - 35127 Padova, Italy*
[d]*DIETI, Università degli studi di Napoli Fedrico II, Via Claudio 21, 80125, Napoli, Italy*

Abstract

The limits for the heat loads on the DEMO first wall are significantly stricter compared to those of ITER due to cooling and breeding blanket requirements. Fast particles in the form of NBI ions can escape the confinement due to magnetic perturbations and produce a significant power load on the first wall. In this contribution, we use the fast ion orbit-following code ASCOT to study NBI losses under the effects of 3D magnetic perturbations, including toroidal field ripple and ferritic inserts. The losses were found to not endanger the integrity of the wall, with loads remaining below 40 kW/m^2 even with unmitigated ripple, and losses did not increase above 2.5 % even with 16 toroidal field coils. Ionization in the scrape-off layer was not found to increase the losses significantly for realistic density profiles, and the design of the wall allows for some flexibility in the distance between the plasma and the first wall tiles.

1. Introduction

Non-axisymmetric magnetic perturbations, such as toroidal ripple due to finite number of toroidal field coils, increase fast particle transport and losses, which can result in localized power loads on plasma facing components [2, 3, 4]. Previous studies for ITER have shown that the power fluxes onto the wall can be substantial, reaching values greater than 100 kW/m^2[5]. Due to the tritium breeding blanket and power exhaust requirements, the peak power loads on the DEMO wall should not exceed 1 MW/m^2 [6], a factor of 2-5 lower than that for the ITER first wall. This includes power loads not only due to fast ions, but also thermal particle and radiative heat fluxes. Thus detailed modeling of fast ion losses in a realistic geometry is vital to ensure that the design is consistent with these engineering requirements.

NBI ion confinement has previously been studied for an earlier iteration of the DEMO design using the Monte Carlo orbit-following code ASCOT [7]. These simulations assumed an axisymmetric, simplified geometry and NBI injectors based on the 1 MeV ITER design. The EU DEMO 2015 features a lower-energy 800 keV injector, which has also previously been studied from the point of view of plasma performance in an axisymmetric case [8]. Thus it is important to study the NBI performance with a realistic geometry and injector design in support of the overall DEMO design effort.

In this contribution we study NBI ion losses during the flat-top phase in the European EU DEMO1 2015 design due to 3D magnetic perturbations, including the toroidal ripple and ferritic inserts. The second section describes the models used for the plasma equilibrium, magnetic field geometry and first wall, contrasting these with the equivalent ITER parameters. The third section presents simulation results for the NBI ion losses while varying the level of ripple mitigation and other factors potentially affecting the losses, such as ionization in the SOL and the shape of the first wall. Finally, in the fourth section the implications of the results on the DEMO design are discussed.

2. DEMO model and simulation configuration

The NBI ion losses were simulated using the ASCOT orbit-following code[11]. The code follows markers representing a fast ion population in a realistic 3D magnetic field and geometry. The markers are followed until they slow down to 1.5 times the local plasma temperature, at which point they are considered thermalized, or until they impact the wall. Guiding center approximation is used until the particles approach within one Larmor radius of the wall, at which point full gyro orbits are simulated to precisely assess the point of impact on the wall.

The plasma equilibrium and the kinetic profiles (figure 1) are based on CRONOS and ASTRA[12] simulations, with a central density of $10.5{\cdot}10^{19}$ m^{-3} and central electron and ion temperatures of 29.5 and 27.5 keV, respectively. The profiles assume a 50-50 mixture of deuterium and tritium, with approximately 8% helium ash and a 0.02% Xenon impurity concentration. Extrapolated profiles in the scrape-off layer are included, corresponding to a SOL density e-folding length of 16 mm. The finite SOL density

Email address: jari.varje@aalto.fi (J. Varje)

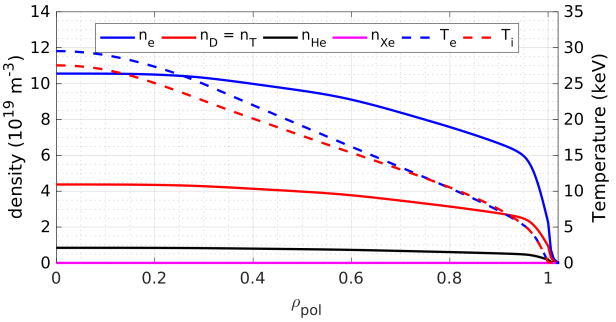

Figure 1: ASTRA-based plasma density and temperature profiles used in the simulations.

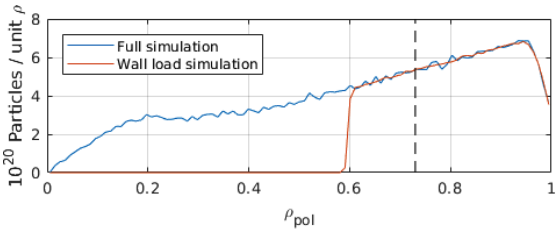

Figure 2: NBI source density as a function of radial coordinate $\rho_{pol} = \sqrt{(\psi - \psi_0)/(\psi_{sep} - \psi_0)}$. Approximate boundary between passing and trapped particles is indicated with the dashed line, corresponding to $|\xi| = 0.56$. Particles born outboard of this line are born on trapped orbits.

allows simulation of NBI particles ionized outside the last closed flux surface (LCFS), which can be rapidly lost due to the unconfined field lines and the proximity to the wall.

The NBI ions were initialized using the beamlet-based Monte Carlo neutral beam code BBNBI[13], which follows the ballistic trajectories of the injected neutral atoms from individual beamlets until they are ionized. The implemented injector geometry was based on the latest DEMO reference design, which consists of 20 modular negative ion sources in two columns with 60 beamlets each [14]. The injection energy is 800 keV and the total power is 16.8 MW per injector. Three injectors are located in adjacent toroidal sectors 20 degrees apart. Simulations were performed for a single NBI injector, and the results were toroidally cloned for the other injectors to represent the full geometry.

The EU DEMO1 2015 design features 18 superconducting toroidal field (TF) coils. A high-resolution TF ripple was calculated using the BioSaw code [15], which integrates the magnetic field from a realistic coil geometry using the Biot-Savart law. The toroidal ripple reaches a value of 0.8 % at the low field side, falling to 0.01 % at the magnetic axis. While the magnetic field and the TF coils are larger in DEMO compared to ITER, the ripple perturbations within the plasma volume are smaller than the corresponding ITER values of 1.1% and 0.015 %. This is due to the favorable plasma position on the high field side, combined with a larger standoff to the coils themselves.

Ferritic inserts (FI), structures of ferritic material located near each TF coil on the low field side, are planned to be used for mitigating the ripple introduced by the finite number of TF coils. The magnetic perturbations due to the ferritic inserts were calculated using the finite-element solver COMSOL. This approach has previously been applied to similar studies in ITER [16, 5]. First, the magnetization of the FI's due to the toroidal field coils and plasma current were calculated. The magnetization was then used to calculate the 3D perturbations within the plasma volume, which was added to the axisymmetric equilibrium field and the TF ripple.

To assess the distribution of particle and energy fluxes on the first wall, a 3D wall mesh was implemented based on a CAD design of the DEMO wall structure. To improve resolution, each flat tile surface was divided into smaller segments, with the final wall model consisting of approximately 200 000 triangles in total. Due to the 18-fold symmetry of both the wall and the 3D magnetic field, the losses were remapped into a single 20 degree sector to improve the statistics for estimating the peak loads.

3. Fast ion losses

Fast ion loss simulations were performed for several different magnetic configurations: an unperturbed axisymmetric equilibrium field, unmitigated toroidal ripple with varying number of TF coils, and ferritic inserts with 25%, 50%, 75% and 100% design mass of ferritic material to assess the efficiency of ripple mitigation.

Initially simulations were performed for all cases with 100 000 markers to identify possible loss regions. After this, larger simulations were performed to improve the statistics on wall load estimates. In the initial simulations, losses were observed only for particles originating outside normalized radial coordinate $\rho_{pol} > 0.6$. Thus for wall load simulations approximately 500 000 markers only born outside this surface were used. While the beam particles are able to penetrate to the magnetic axis and beyond, the number of ionized particles peaks near the edge of the plasma (figure 2). This is due to the high pedestal density combined with the 800 keV beam energy. However, the shine-through losses are negligible for the same reasons [8, 9]. Particles ionized outside approximately $\rho_{pol} > 0.73$, corresponding to $|\xi| < 0.56$, become trapped on banana orbits, while particles deeper inside are born on passing orbits.

3.1. NBI ion confinement

The confinement of the NBI ions was found to be excellent in all cases, with losses of less than 0.3% of total injected power even in the unmitigated ripple configuration (Table 1). Including the ferritic inserts at full design mass further reduces the losses to 2 kW, nearly to the level of the unperturbed axisymmetric case. Reducing the mass of the ferritic inserts reduces the saturated magnetization and thus the ripple mitigation. However, already at 25

Table 1: NBI ion losses for the axisymmetric 2D equilibrium, unmitigated ripple and ferritic insert configurations.

Configuration	NBI losses
Unmitigated Ripple 16 coils	609 kW
Unmitigated ripple 18 coils	49 kW
Ripple + 25 % FI mass	19 kW
Ripple + 50 % FI mass	8 kW
Ripple + 75 % FI mass	3 kW
Ripple + ferritic inserts	1 kW
2D equilibrium	< 1 kW

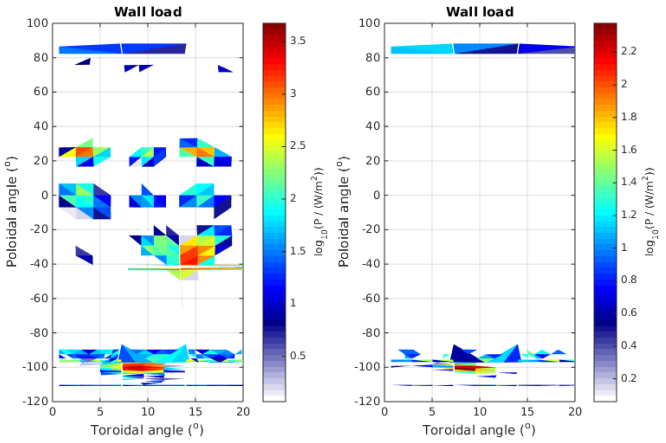

Figure 3: Wall power loads mapped into a single 20^o sector in the unmitigated ripple case (top) and in the ferritic insert case (bottom).

% of design mass the ferritic inserts reduce the losses by half. 50 % mass FI's reduce the losses by nearly an order of magnitude.

As the confinement in the design configuration with 18 TF coils is excellent, a simulation was performed for a case with 16 TF coils, where the coil current was scaled up to match the on-axis toroidal field value of the original design. The increased ripple increases to losses by an order of magnitude to 609 kW, but this still represents only 2.3 % of the total injected power.

3.2. Loss mechanisms and wall loads

In the unmitigated ripple case, the NBI ion losses are primarily concentrated around the outer midplane and the divertor (figure 3). Additionally, some particles impact the wall near the top of the machine, while some are lost to the baffle at divertor entrance. The losses on the main chamber wall correspond to locations where the distance between the LCFS and the wall are smallest. The losses at the outer midplane are eliminated with the inclusion of FI's. The peak wall loads remain below 40 kW/m^2 even in the unmitigated ripple configuration.

The majority of NBI ions are born close to the edge of the plasma due to the 800 keV injection energy and high density. However, first orbit losses are nearly non-existent: all lost particles have already slowed down considerably and take a minimum of 10^{-3} s to reach the wall.

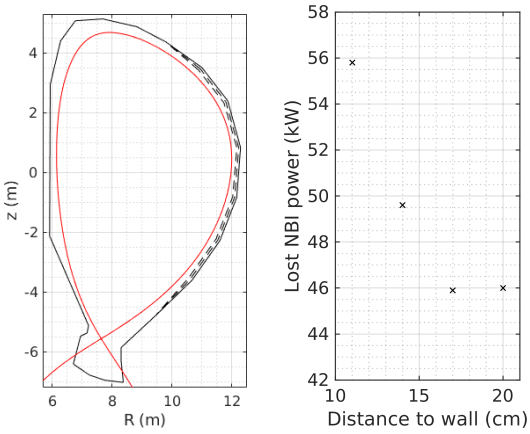

Figure 4: NBI losses as a function of distance between the LCFS and the wall at the outer midplane (right) for a range of wall contours (left).

The losses at the top of the machine and the two tiles at and above the outer midplane have similar pitch distribution, peaking around $\xi = -0.2$. These are ripple-enhanced diffusive losses of deeply trapped banana orbits.

The losses below the outer midplane and at the divertor baffle are concentrated around pitch $\xi = 0$, suggesting the losses in this region are due to local ripple well trapping. However, the particles have already slowed down to energies below 400 keV before becoming trapped and are rapidly transported downwards to the wall by the ∇B drift.

Finally, the losses in the divertor region are concentrated near thermal energies, indicating these are primarily diffusive losses from deeper inside the plasma.

3.3. Reduced wall clearance

To evaluate the effect of the clearance between the plasma and the first wall on the losses, a scan of wall configurations with reduced clearance was performed. A 2D contour representing the innermost limiting points of the 3D wall structure was used for these cases. The distance between the wall and the separatrix on the outboard side near outer midplane was linearly scaled between 10 cm and the reference value of 25 cm.

At the closest distance, the losses are approximately 25 % higher compared to the reference design (Figure 4). As the distance is increased beyond 20 cm, the losses saturate to a value close to the reference case. The 6% difference between the 2D and 3D cases is due to the 3D structure of the wall, which enables some particles to pass in the recesses between the first wall tiles.

3.4. SOL ionization

While the majority of the particles penetrate deep into the plasma due to the gradual pedestal shape and high beam energy, some particles are ionized already in the scrape-off layer due to the finite density there. To evaluate the effect of these losses, the decay of density in the SOL

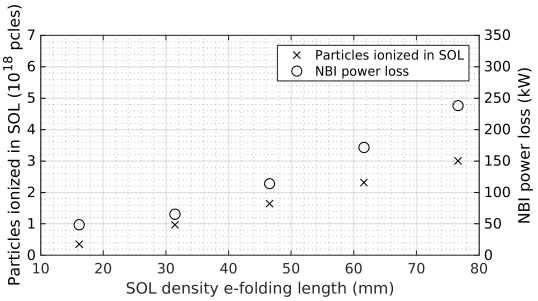

Figure 5: Particles ionized in the scrape-off layer (left) and NBI losses (right) with increasing SOL density decay length.

was changed by adjusting the e-folding or decay length of the density from the reference value of 15 mm upwards (Figure 5).

The fraction of particles ionized in the SOL increases linearly as more particles are ionized closer to the edge and are lost faster. The losses increase significantly beyond a decay length of 40-50 mm. This is due to particles born on orbits that are immediately lost to the wall, increasing the wall loads in the region near the injection point. However, such high decay lengths and SOL densities are likely unrealistic, but with a reduced wall clearance even moderate increases in the SOL density might become significant.

4. Summary and discussion

Despite the increased power and stricter engineering constraints for first wall power loads in the European DEMO design compared to ITER, NBI ion losses are not expected to pose a concern to the integrity of the plasma facing components. Based on 3D ASCOT simulations, total losses remain below 0.3% of the injected power of 50 MW, and peak wall loads do not exceed 40 kW/m^2 even with unmitigated toroidal field ripple perturbations. This is well below the engineering limits of 1 MW/m^2. The ripple-mitigating ferritic inserts reduce the losses nearly to the level of unperturbed axisymmetric field. Even with a configuration with only 16 TF coils and no ripple mitigation, the losses remain below 2.3 %.

Features aiding the NBI confinement in DEMO include a favorable coil geometry, where the plasma is located on the high field side of the coils, reducing the maximum TF ripple within the plasma volume to 0.8% compared to ITER values of 1.1%. Additionally, the shallow pedestal density profile allows deeper beam penetration despite the reduced NBI energy of 800 keV compared to ITER injection energy of 1 MeV. Combined with a larger standoff distance between the last closed flux surface and the first wall, this minimizes prompt high-energy losses. Instead, the losses are due to ripple-enhanced diffusion, with the strike locations in some cases affected by local ripple well trapping.

Based on the simulation results, NBI ion losses in the European DEMO are not a concern for machine protection or plasma performance during flat-top operation. The good confinement with unmitigated ripple suggests that the ferritic inserts may not even be needed, and even a 16 coil design might be sustainable, at least from the point of view of NBI ion confinement. However, these simulations assume only perturbations due to the toroidal field ripple and ferritic inserts in the vacuum approximation. Other perturbations, such as mitigation of edge localized modes with resonant magnetic perturbations imposed with external ELM control coils (ECC) can dramatically increase the losses. In previous simulations for ITER the losses have been observed to reach up to 4% of the injected power. Furthermore, the response of the plasma to the external perturbations can change and redistribute the losses [17].

Finally, the simulations assume only neoclassical transport in a quiescent plasma with no sawtooth, NTM, TAE or other fast particle instabilities. While the plasma performance required in DEMO does not allow for significant instabilities, these can redistribute the fast ions and possibly increase the losses. Simulations with these perturbations will follow once the DEMO design has converged and detailed plasma simulations become relevant.

This work has been carried out within the framework of the EUROfusion Consortium and has received funding from the Euratom research and training programme 2014-2018 under grant agreement No 633053. The views and opinions expressed herein do not necessarily reflect those of the European Commission. This work was partially funded by the Academy of Finland project No. 259675, and has also received funding from Tekes – the Finnish Funding Agency for Innovation under the FinnFusion Consortium. The work was carried out using the HELIOS supercomputer system at International Fusion Energy Research Centre, Aomori, Japan, under the Broader Approach collaboration between Euratom and Japan, implemented by Fusion for Energy and JAEA. The supercomputing resources of CSC - IT center for science were utilised in the studies. Some of the calculations were performed using computer resources within the Aalto University School of Science "Science-IT" project.

[1] R. Wenninger et al. 2017 Nucl. Fusion 57 016011
[2] K. Shinohara et al. 2011 Fusion 51 063028
[3] T. Kurki-Suonio et al. 2009 Nucl. Fusion 49 095001
[4] R. Akers et al. 2016 In Proc. 26th IAEA Fusion Energy Conference, 17-22 October 2016, Kyoto, Japan, TH/4-1
[5] T. Kurki-Suonio et al. 2016 Nucl. Fusion 56 112024
[6] R. Wenninger et al. 2017 Nucl. Fusion 57 046002
[7] O. Asunta et al. 2015 In Proc. 42nd EPS Conference on Plasma Physics, 22-26 June 2015, Lisbon, Portugal, P2.156
[8] P. Vincenzi et al. 2017 In Proc. 44th EPS Conference on Plasma Physics, 26-30 June 2017, Belfast, UK, P4.146
[9] P. Vincenzi et al. 2018 In Proc. 23rd International Conference on Plasma Surface Interactions in Controlled Fusion Devices, 18-22 June 2018, Princeton, USA, poster 488
[10] D. Pfefferlé et al. 2016 Nucl. Fusion 56 112002
[11] E. Hirvijoki et al. 2014 Comput. Phys. Commun. 185 1310-1321
[12] E. Fable et al. 2017 Nucl. Fusion 57 022015
[13] O.Asunta et al. 2015 Comput. Phys. Commun. 188 33-46
[14] P. Sonato et al. 2017 Nucl. Fusion 57 056026
[15] S. Äkäslompolo et al. 2015 Fusion Eng. Des. 98-99 1039-1043
[16] S. Äkäslompolo et al. 2015 Nucl. Fusion 55 093010
[17] J. Varje et al. 2016 Nucl. Fusion 56 046014